



# Gasoline aromatics: a critical determinant of urban secondary organic aerosol formation

Jianfei Peng<sup>1,a</sup>, Min Hu<sup>1,4</sup>, Zhuofei Du<sup>1</sup>, Yinhui Wang<sup>2</sup>, Jing Zheng<sup>1</sup>, Wenbin Zhang<sup>2</sup>, Yudong Yang<sup>1</sup>, Yanhong Qin<sup>1</sup>, Rong Zheng<sup>2</sup>, Yao Xiao<sup>1</sup>, Yusheng Wu<sup>1</sup>, Sihua Lu<sup>1</sup>, Zhijun Wu<sup>1</sup>, Song Guo<sup>1</sup>, Hongjun Mao<sup>3</sup>, and Shijin Shuai<sup>2</sup>

<sup>1</sup>State Key Joint Laboratory of Environmental Simulation and Pollution Control, College of Environmental Sciences and Engineering, Peking University, Beijing 100871, China

<sup>2</sup>State Key Laboratory of Automotive Safety and Energy, Tsinghua University, Beijing 100084, China

<sup>3</sup>College of Environmental Sciences and Engineering, Nankai University, Tianjin 300071, China

<sup>4</sup>Beijing Innovation Center for Engineering Science and Advanced Technology, Peking University, Beijing 100871, China

<sup>a</sup>now at: Department of Atmospheric Sciences, Texas A&M University, College Station, TX 77843, USA

Correspondence to: Min Hu (minhu@pku.edu.cn) and Shijin Shuai (sjshuai@tsinghua.edu.cn)

Received: 19 March 2017 – Discussion started: 27 March 2017

Revised: 27 July 2017 – Accepted: 15 August 2017 – Published: 13 September 2017

**Abstract.** Gasoline vehicle exhaust is an important contributor to secondary organic aerosol (SOA) formation in urban atmosphere. Fuel composition has a potentially considerable impact on gasoline SOA production, but the link between fuel components and SOA production is still poorly understood. Here, we present chamber experiments to investigate the impacts of gasoline aromatic content on SOA production through chamber oxidation approach. A significant amplification factor of 3–6 for SOA productions from gasoline exhausts is observed as gasoline aromatic content rose from 29 to 37 %. Considerably higher emission of aromatic volatile organic compounds (VOCs) using high-aromatic fuel plays an essential role in the enhancement of SOA production, while semi-volatile organic compounds (e.g., gas-phase PAHs) may also contribute to the higher SOA production. Our findings indicate that gasoline aromatics significantly influence ambient PM<sub>2.5</sub> concentration in urban areas and emphasize that more stringent regulation of gasoline aromatic content will lead to considerable benefits for urban air quality.

## 1 Introduction

Fossil-fuel-powered vehicles, an important source of NO<sub>x</sub>, volatile organic compounds (VOCs) and atmospheric particulate matter (PM), are always associated with severe haze

events, human health risks and climate forcing, particularly in urban areas (Parrish and Zhu, 2009; Guo et al., 2014; Huang et al., 2014; Kumar et al., 2014; S. Liu et al., 2015; Kelly and Zhu, 2016; Peng et al., 2016b). Gasoline is the most widely used vehicle fuel and accounts for the largest total transportation energy consumptions in many countries, e.g., the USA and China (NBSC, 2015; EIA, 2017). Among all the gasoline-related PM components, secondary organic aerosol (SOA) produced via atmospheric oxidation of VOC precursors in the exhaust has been proved by chamber experiments to be a large fraction, if not the largest, of gasoline vehicular PM (Zervas et al., 1999; Jimenez et al., 2009; Gordon et al., 2014a; Jathar et al., 2014; Platt et al., 2014; T. Liu et al., 2015). Moreover, ambient measurement also demonstrated that gasoline SOA was the largest source of vehicular carbonaceous PM in megacities such as Los Angeles (Bahreini et al., 2012). However, although increasingly stringent gasoline fuel standards, especially on sulfur content, have been implemented in the past decades in many countries to reduce the emissions, the impacts of fuel compositions on SOA production have not been sufficiently taken into account in the current gasoline fuel standards. This deficiency is mainly attributed to the poor understanding of the effects of fuel properties on the related SOA formation, and may ultimately lead to a policy bias on the control of vehicle emission regarding the reduction of atmospheric pollution.

Aromatic hydrocarbons, which are unsaturated compounds with at least one benzene ring, account for 20–40 % *v/v* of gasoline fuel. Aromatic VOCs (e.g., toluene, xylenes and trimethylbenzenes) react exclusively with the OH radical in the atmosphere, leading to the formation of a variety of semi- or low-volatility species (e.g., benzoic acid) (Zhang et al., 2015; Schwantes et al., 2017), which will partition onto existing particles and be recognized as anthropogenic SOA. Therefore, the higher emission of aromatic VOCs will likely result in more SOA formation potential. Existing fuel-effect experimental and model studies have shown that high-aromatic fuel in gasoline fuel will lead to more emissions of primary PM as well as some aromatic VOCs (Zervas et al., 1999; EPA, 2013; Karavalakis et al., 2015; Wang et al., 2016), indicating the considerable potential impact of gasoline aromatic content on SOA production. Furthermore, though aromatic content in diesel fuel may have an insignificant impact on SOA formation (Gordon et al., 2014b), SOA production from gasoline vehicle is considered more sensitive to aromatic content than that from diesel vehicle (Jathar et al., 2013). However, until now, very few studies have successfully quantified the impact of gasoline aromatic content on SOA production and directly revealed the possible pathway.

In this study, in-depth, comprehensive research was conducted to investigate the link between gasoline fuel compositions, primary gas- and particle-phase emission, and corresponding SOA formation. Gasoline exhaust emissions were examined on two platforms under two different conditions. The first platform was a chassis dynamometer system equipped with a constant-volume sampler (CVS). Vehicle exhausts after CVS were introduced into an outdoor environmental chamber and subjected to aging under typical polluted urban conditions to simulate the SOA formation in the ambient atmosphere. The second platform was an experimental engine system on which emissions from a port gasoline injection (PFI) engine and a gasoline direct injection (GDI) engine were examined. SOA formation experiments from engine exhausts were carried out with relatively high OH exposure compared to ambient conditions to obtain the SOA production potential. Most importantly, different gasoline fuels blended from different refinery streams were utilized in both platforms to probe the critical link among fuel components, VOC emissions and related SOA production.

## 2 Materials and methods

### 2.1 Test fleet, cycle and engine

A commercial PFI vehicle, an experimental PFI engine and a GDI engine were tested in this work.

The chosen PFI vehicle was a commonly used vehicle model in China that was certified to the China IV emission standard (equivalent to Euro 4). The mileage of the test ve-

hicles was about 3000 km. The fleet was driven on a chassis dynamometer system (Burke E. Porter Machinery Company) using a cold-start Beijing cycle in order to better simulate the actual driving situation in Beijing. The Beijing cycle was about 17 min long, with a highest speed of about 50 km h<sup>-1</sup> (Fig. S1 in the Supplement). The temperature and the absolute humidity in the dynamometer room were kept at 23.0 ± 1.0 °C and 8.4 ± 0.9 g m<sup>-3</sup>, respectively, for all vehicle experiments (Table S1 in the Supplement).

Vehicle exhaust underwent the first stage of dilution with filtered ambient air using a CVS operated at 5.5 m<sup>3</sup> min<sup>-1</sup> for all experiments. Approximately 5.3 L min<sup>-1</sup> of diluted exhaust from the CVS was introduced into the 1.2 m<sup>3</sup> chamber to be further diluted with the clean air in the chamber (Fig. 1). The average dilution factor was approximately 20 in the CVS and was approximately 15 in the chamber. During the entire cycle, a light-duty gasoline vehicle emissions testing system (Horiba, Ltd.) was used to measure the average and real-time concentration of THC, CO<sub>2</sub>, CO and NO<sub>x</sub>. In addition, a filter-based sampler (AVL SPC 472) was used to sample primary particles from gasoline vehicles for chemical composition analysis.

The PFI and GDI engines were manufactured by a domestic Chinese automaker and equipped with a turbocharger together with downsized displacement. The PFI engine used in this study was an experimental one with an old three-way catalyst (TWC), while the GDI engine was a commercial one designed for vehicles meeting the China IV emission standard. The operation mode of the PFI and GDI engine for chamber experiments was 2000 rpm with 50 % load. After the engine became stable in this operating mode, the exhaust was introduced into the chamber passing through a heater (150 °C) and a filter, with a flow rate of 5 L min<sup>-1</sup> and an injection time of 1 min. Particle number, mass and chemical composition, and VOCs in the exhaust were characterized in the same operating mode. Primary particles were sampled by a filter-based sampler (AVL SPC 472) and particulate chemical compositions, i.e., ions, EC, OC and polar and nonpolar organic species, were analyzed using ion chromatography, an EC/OC analyzer (Sunset Laboratory Inc.) and gas chromatography–mass spectrometry (GC-MS) (Guo et al., 2013), respectively. A detailed description of the engine experiments can be found in our previous study (Du et al., 2017), and all engine experiments used in this study are illustrated in Table S2.

### 2.2 Fuels

Three fuels (F1, F2 and F3) were utilized in this study to investigate the impacts of the gasoline fuel on SOA formation. A commercial phase V gasoline (F1 fuel) with equivalent octane number of 93 was used as the base fuel. F1 fuel contains 29.8 % aromatics and 4.1 % olefin content (Table 1). The most abundant species in Fuel 1 was *i*-pentane, followed by toluene and 2-methylpentane (Table S3).

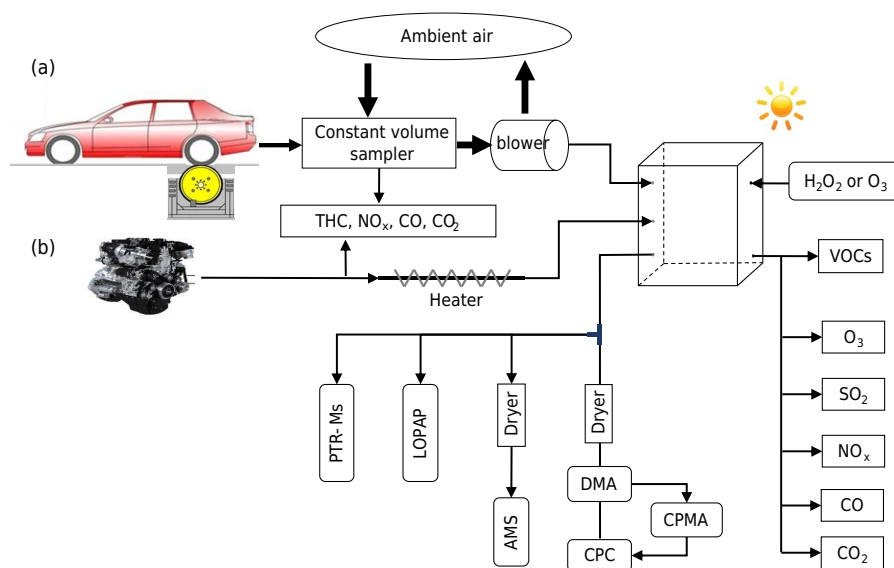


**Figure 1.** Schematic diagram of chamber experiments.

F2 fuel was blended from 80 % of F6 fuel and 20 % of refinery catalytic stream. Octane (18.8 %) and aromatic content (28.5 %) in F2 fuel are very similar to that in F1 fuel, with the only difference being the olefin content.

F3 fuel was blended from 80 % F2 fuel and 15–20 % refinery reformat stream with high aromatic content and a very small amount of *o*-octane and *n*-heptane to keep the same octane level. Compared with F2 fuel, F3 fuel contained similar olefin content (15.4 %) but higher aromatic content (36.7 %) (Table 1). In particular, much higher toluene, ethylbenzene and methylethylbenzene were found in F3 fuel (Table S3). Both F2 and F3 fuels meet the phase V gasoline standard. On the basis of the aromatic contents, the F2 and F3 fuel can be well representative of the fuel normally used around year 2010 and after 2013, respectively, on the Chinese market, such as in Beijing and Shanghai.

### 2.3 Chamber simulation

The quasi-atmospheric aerosol evolution study (QUALITY) chamber was utilized to quantify SOA formation from both gasoline engine exhaust and gasoline vehicle exhaust. The 1.2 m<sup>3</sup> two-layer chamber is composed of an inner layer of 0.13 mm PFA Teflon and an outer, rigid, 5.6 mm thick acrylic shell (Cyro Industries Acrylite, OP-4). Both layers allowed for efficient transmission of sunlight in UV ranges (Peng et al., 2016b). Pre-experiments showed that wall loss decreased the particle number concentration by about 50 % in about 3.5 h. SO<sub>2</sub> and NO<sub>x</sub> decreased to about 50 % after 20 h, while toluene and isoprene did not show obvious wall loss during a 2-day experiment (Peng et al., 2017).

Prior to each experiment, the QUALITY chamber was covered with two layers of anti-UV cloth to shield the cham-

**Table 1.** Parameters of the tested fuels.

Specifications	F1 (base)	F2	F3
Research octane number	93.1	93.6	93
Motor octane numbers	86.3	84.8	84
Density (g mL <sup>-1</sup> )	0.72	0.728	0.744
Rvp (kPa)	58.6	63.2	55.4
Aromatics (% v/v)	29.8	28.5	36.7
Olefin (% v/v)	4.1	18.8	15.4
Ethanol (% v/v)	< 0.1	0.12	0.01
Oxygen (% m/m)	0.01	0.06	0.02
Mn (mg kg <sup>-1</sup> )	< 0.1	< 0.1	< 0.1
Sulfur (mg kg <sup>-1</sup> )	9	7	6
T10 (°C)	50.8	50.9	55.4
T50 (°C)	79.4	101.9	109.9
T90 (°C)	162.6	167.5	164.3
Fbp (°C)	187.9	195.7	194.4
Quality level	China phase V	China phase V	China phase V

ber from sunlight and flushed by zero air with a flow rate of 10 L min<sup>-1</sup> for more than 15 h to ensure clean conditions. In both vehicle and engine experiments, excess (1 mL, 30 % v/v) H<sub>2</sub>O<sub>2</sub> was also injected into the chamber via the makeup zero air as an extra hydroxyl radical (OH) source after adding the exhaust. Chamber experiments were normally conducted from noon to late afternoon, with an inside temperature of 30–35 °C and relative humidity (RH) of 40–60 %. A suite of high-time-resolution state-of-the-art aerosol instruments were utilized to measure the gas concentration and a comprehensive set of particle properties throughout the experiments, including concentrations of HONO, SO<sub>2</sub>, NO<sub>x</sub>, O<sub>3</sub>, CO, CO<sub>2</sub> and several VOCs and the particle diameter, mass, and chemical composition (Fig. 1 and Table S4).

Particle number distributions were measured with a scanning mobility particle sizer (SMPS) system, which was composed by one differential mobility analyzer (DMA, TSI,

Inc., model 3081) and one condensation particle counter (CPC, TSI, Inc., model 3772). The mass concentration and size distribution of particle chemical compositions, including organic aerosol (OA), sulfate, nitrate, ammonium and chloride, were measured by a high-resolution time-of-flight aerosol mass spectrometer (HR-ToF-AMS, Aerodyne Research, Inc.). The evolution of several VOCs was measured continually by a proton transfer reaction mass spectrometer (PTR-MS, Ionicon). Dedicated gas monitors, including the  $\text{SO}_2$ ,  $\text{NO}_x$ , CO,  $\text{CO}_2$  and  $\text{O}_3$  monitors (Thermo Inc.), were utilized and calibrated each experiment day. VOCs in the chamber were also sampled by canisters every 1 h during vehicle experiments and analyzed with a GC-MS/FID system (Wang et al., 2015).

Zero airflow was connected to the chamber over the entire experiment to make up the volume of air withdrawn by the instruments. To minimize the sampling volume by the instruments, all instruments except SMPS were connected with several three-way valves, which were successively switched between the ambient air and the chamber every 15 or 30 min.

### 3 Results

#### 3.1 Simulation of SOA formation from gasoline exhausts

The temporal evolution of gas- and particle-phase species during the chamber experiment is illustrated in Fig. 2. The initial concentrations of  $\text{NO}_x$ , benzene and toluene in the chamber were 163, 5.6 and 16.8 ppb, respectively, corresponding to the severe urban haze condition in the megacities (Guo et al., 2014). After the chamber was exposed to sunlight, 99 % of NO was converted to  $\text{NO}_2$  within the first 10 min. This is because the fast photolysis of  $\text{H}_2\text{O}_2$  produced a large amount of OH radical and further  $\text{HO}_2/\text{RO}_2$  radicals inside the chamber, which reacted with NO to form  $\text{NO}_2$  (Seinfeld and Pandis, 2006). Then, the concentration of  $\text{O}_3$  increased rapidly to approximately 400 ppb after 1 h exposure, and gradually decreased later in this experiment (Fig. 2a).

Over the entire experiment, benzene and toluene experienced a gradual decay in the concentrations, but with different decay coefficients (Fig. 2b). Aerosol evolution is always characterized by a photochemical-age-based parameterization method in ambient measurements as well as chamber experiments (Hu et al., 2013; de Gouw et al., 2005; Peng et al., 2016a). Therefore, in order to compare our SOA productions in different experiments (in which solar flux was different), OH exposures were calculated based on the ratios of benzene and toluene concentrations, which reacted at different rates with OH radical (de Gouw et al., 2005). In addition, to compare the OH exposure in our chamber experiments with the previous ambient measurements, the OH concentration in the ambient air was assumed as  $1.6 \times 10^6 \text{ molec cm}^{-3}$  (Hu et al., 2013; Peng et al., 2016a), and the equivalent photo-

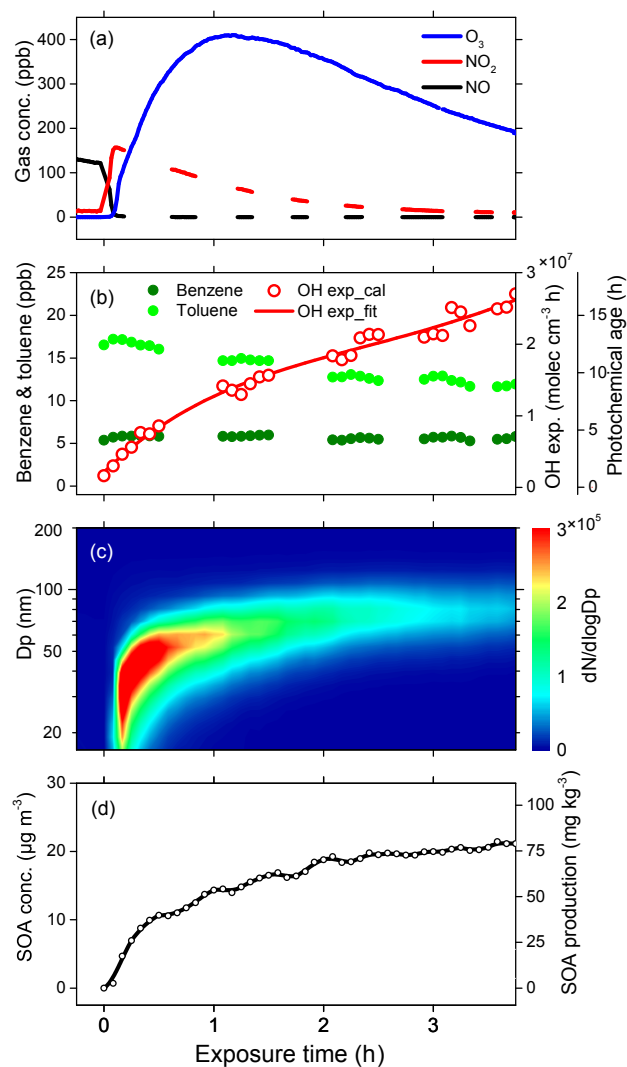


**Figure 2.** Evolution of gas-phase species (a, b), particle size distribution (c), and SOA concentration and production (d) during a typical chamber experiment (V2). OH exposure and photochemical age are calculated based on the ratios of benzene and toluene concentrations, assuming that OH concentration is  $1.6 \times 10^6 \text{ molec cm}^{-3}$ . The SOA mass concentration is obtained by intergrading size distribution of particles inside the chamber on the basis of measured particle density. The measured SOA mass concentration is corrected according to the particle wall loss curve as well as the dilution effect for both particles and gas precursors.

chemical ages of chamber experiments were then estimated by the ratio of OH exposure in the chamber to the assumed OH concentration in the ambient air.

New particle formation occurred inside the chamber within 10 min of exposure to sunlight (Fig. 2c). These newly formed particles performed as seeds for the further formation of secondary species. A large quantity of secondary aerosols was then formed in the chamber, leading to the fast growth in the diameter of these particles to approximately 70 nm af-

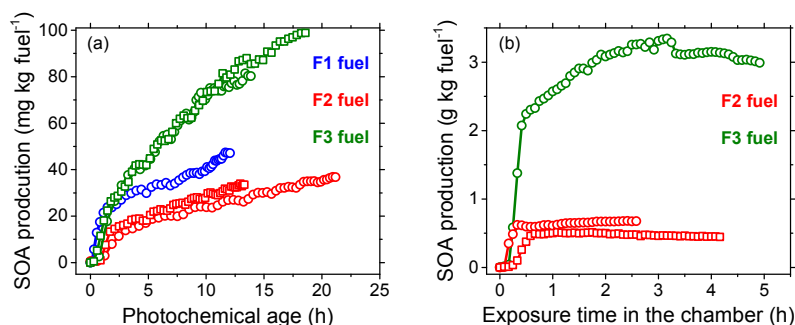


**Figure 3.** SOA production in the vehicle experiments as a function of photochemical age (a) and in the engine exhaust experiments as a function of exposure time (b). The green squares, green circles, red squares, red circles and blue circles (a) represent experiments V1, V2, V3, V4 and V5 shown in Table S1, respectively. The green circles, red squares and red circles (b) represent experiments E1, E2 and E3 shown in Table S2, respectively.

ter 3 h of aging. The measurement of the particle compositions by the AMS reveals that the largest mass fraction of secondary aerosols in the chamber was SOA (approximately 95 %, Fig. S2), indicating the critical role of the SOA for the secondary aerosol formation from gasoline exhausts. Because of the low aerosol loading (initially lower than  $2 \mu\text{g m}^{-3}$ ) and low relative humidity (40–50 %) inside the chamber, heterogeneous reactions and aqueous-phase processing were not important for the formation of SOA in this study (Zhang et al., 2015). Furthermore, the O : C ratio of SOA formed in the chamber stayed stable around 0.4 over the entire experiment, indicating that condensed-phase reactions, i.e., aqueous or heterogeneous reactions, which produce highly oxidized oligomers, were not significant in the chamber experiments in this study. The SOA, therefore, was likely formed via condensation of less volatile products oxidized through gas-phase reactions of VOC precursors with limited multigenerational chemistry (Robinson et al., 2007; Jimenez et al., 2009; Jathar et al., 2014). The AMS spectrum profile of gasoline SOA obtained in this study was highly correlated with the ambient less-oxidized secondary organic aerosol (LO-OOA) in Beijing ( $R^2 = 0.99$ , Fig. S3), further confirming the important contribution of gasoline emission on ambient  $\text{PM}_{2.5}$ .

SOA productions per fuel consumption or mileage were calculated on the basis of SOA mass concentration inside the chamber, dilution factors both in the CVS and inside the chamber, and fuel consumption/mileage of our working cycle. SOA mass concentration inside the chamber was corrected according to the particle wall loss curve (Fig. S4) as well as the dilution effect of both particles and gas precursors due to the continuous zero air flow into the chamber to make up the sampling volume (Fig. S5). SOA production at the end of this experiment was calculated to be  $80 \text{ mg kg-fuel}^{-1}$ , or  $6.7 \text{ mg km}^{-1}$ , after 3.5 h of aging (Fig. 2d). These values were 6.8 times higher than the emission factors (EFs) of primary particles (including both primary organic matters and elemental carbon) at the same cycle.

### 3.2 Fuel impacts on SOA production

The average fuel consumptions per unit distance using F1, F2 and F3 fuels were 0.113, 0.112 and  $0.113 \text{ L km}^{-1}$ , respectively, indicating no difference in fuel economy among the three fuels. On the other hand, high-aromatic-content gasoline led to noticeably large enhancement on SOA production from both vehicle and engine experiments. As illustrated in Fig. 3a, the final SOA production from gasoline vehicle exhaust ranged from 30 to  $98 \text{ mg kg-fuel}^{-1}$  at the end of each experiment, comparable to the results from cold-start experiments in previous studies (Gordon et al., 2014a; Jathar et al., 2014). Experiments using F3 fuel (with 36.7 % v/v aromatic content) exhibit the highest SOA production factors, followed by F1 fuel (with 29.8 % v/v aromatics content) and F2 fuel (with 28.5 % v/v aromatics content). The average SOA production at 12 equivalent photochemical hours using F3 fuel was  $76 \text{ mg kg-fuel}^{-1}$  ( $6.3 \text{ mg km}^{-1}$ ), equivalent to 3 times that using F2 fuel ( $25 \text{ mg kg-fuel}^{-1}$ ,  $2.1 \text{ mg km}^{-1}$ ). Additionally, we observed much larger amount of the SOA formation in the first few photochemical hours in all experiments. The average production rates of SOA were as high as  $5\text{--}13 \text{ mg kg}^{-1} \text{ h}^{-1}$  over each experiment, suggesting that the first-generation oxidation of some precursors inside the chamber produced a large amount of SOA. This indicated the existence of some semi-volatile organic compounds (SVOCs) (Robinson et al., 2007; Keyte et al., 2013). It is worth noting that the higher VOC and SOA concentrations inside the chamber in the F3 fuel experiments might lead to more SVOCs partitioning onto particles. This partitioning, however, would not qualitatively change the experiment conclusion that higher fuel aromatics led to higher SOA production.

SOA formation experiments from the PFI engine exhaust were conducted under high oxidizing conditions to obtain the SOA formation potential. As illustrated in Fig. 3b, most of the SOA was formed within the first half hour of each engine experiment and very little increase was observed over